Article

Effect of Grain Size on the Friction-Induced Martensitic Transformation and Tribological Properties of 304 Austenite Stainless Steel

Bo Mao [1,2,*] **, Shuangjie Chu** [1,2,*] **and Shuyang Wang** [1]

[1] Baoshan Iron & Steel Cooperation Limited, Shanghai 201900, China; wangshuyang@baosteel.com
[2] School of Materials Science and Engineering, Shanghai Jiao Tong University, Shanghai 200240, China
* Correspondence: bmao@nevada.unr.edu (B.M.); sjchu@baosteel.com (S.C.); Tel.: +01-775-223-0807 (B.M.); +86-21-2065-8818 (S.C.)

check for
updates

Abstract: Friction and wear performance of austenite stainless steels have been extensively studied and show a close relationship with the friction-induced martensitic transformation. However, how the grain size and associated friction-induced martensitic transformation behavior affect the tribological properties of austenite steels have not been systematically studied. In this work, dry sliding tests were performed on an AISI 304 stainless steel with a grain size ranging from 25 to 92 μm. The friction-induced surface morphology and microstructure evolution were characterized. Friction-induced martensitic transformation behavior, including martensite nucleation, martensite growth and martensite variant selection and its effect on the friction and wear behavior of the 304 stainless steel were analyzed. The results showed that both the surface coefficient of friction (COF) and the wear rate increase with the grain size. The COF was reduced three times and wear rate was reduced by 30% as the grain size decreased from 92 to 25 μm. A possible mechanism is proposed to account for the effect of grain size on the tribological behavior. It is discussed that austenite steel with refined grain size tends to suppress the amount of friction-induced martensitic transformed and significantly alleviates both the plowing and adhesive effect during dry sliding.

Keywords: austenite stainless steels; friction; wear; grain size; martensitic transformation

1. Introduction

Austenite stainless steels with low stacking fault energy (SFE) have been widely used in structural applications due to their good combination of strength and ductility, excellent corrosion resistance, and desirable weldability [1]. It was widely assumed that their excellent combination of strength and ductility is through the transformation-induced plasticity (TRIP) effect, in which the metastable austenite transforms to martensite upon plastic deformation [2]. Stress or stain-induced martensitic phase transformation has been extensively identified in the austenite stainless steels during their sheet forming and crash applications, and significantly affects their engineering performance [3].

Tribological performance in terms of friction and wear is an important property in the manufacturing and applications of austenite stainless steels, particularly for mechanical components subjected to sliding motion, such as bearing, pistons, and valves, in medical, marine and automotive applications which require both high bearing strength and good corrosion resistance [4,5]. Moreover, friction and wear are also important concerns during the forming processes of austenite stainless steels [6,7]. It is fundamentally assumed that friction and wear behaviors are results of materials' responses to localized deformation [8,9]. Therefore, friction-induced martensitic transformation plays an important role on the friction and wear behavior austenite stainless steels involving the TRIP

effect [7,10]. Several studies have been carried out to investigate the relationship between their tribological properties and friction-induced martensitic transformation. For instance, Yang et al. [7] reported that the friction-induced martensitic transformation in a 304 stainless steel affected the formation and composition of the wear debris and the nature of the transfer layer. Hua et al. [11] showed that adhesion wear mechanism dominated during the dry sliding of a 304 stainless steel due to the interaction between hard pin material and freshly produced martensite. Recently, Lee et al. [12] demonstrated that the specific wear rates of SUS304 and 316 stainless steels, as well as the volume of friction-induced martensite increased with the sliding speed.

Despite these research efforts, little attention has been paid to investigate the initial austenite grain size on the friction and wear behavior of austenite steels. Since the deformation induced martensite nucleates mostly from the intersections of shear bands [13,14] whose activities are strongly affected the austenite grain size, it was widely accepted that the stress-induced martensite formation has a strong grain size dependence [15,16]. Jin et al. [17] showed that grain refinement in a Fe-Cr-Ni alloy increases the stability of austenite and leads to the delay of martensitic transformation. Varma et al. [18] demonstrated that the stress-induced martensitic transformation in a 304 steel was sensitive to the parent austenite grain size, a finer grain resulting in a higher volume of martensite transformed. Therefore, it is expected that the initial grain size of austenite stainless steel has a prominent impact on the friction-induced martensitic transformation, and influence its tribological properties. Recently, Bregliozzi et al. [19] showed that a refined grain size in a 304 stainless steels results in an improved wear resistance. However, the detailed mechanism involving the martensitic transformation was not analyzed.

Therefore, understanding the relationship among the austenite grain size, friction-induced martensitic transformation behavior and tribological performance of austenite stainless steels is of significantly importance. This research aims to investigate the effect of grain size on the friction and wear behavior of austenite stainless steels, with a particular focus on the friction-induced martensitic transformation behavior. AISI 304 stainless steel samples with various initial grain sizes were prepared. Sliding tests under dry condition were conducted for friction and wear property evaluation. The surface coefficient of friction (COF) values and 3-D morphology of the wear tracks were measured. The friction-induced martensitic transformation was characterized and analyzed. The relationship among the austenite grain size, martensitic transformation behavior and tribological performance of 304 stainless steels was discussed. A possible mechanism responsible for the effect of austenite grain size on the friction-induced martensite transformation and tribological performance of austenite steels was proposed. It was found that austenite grain size has a significant impact on the friction-induced martensitic transformation behavior and therefore affects both the surface COF and wear resistance of 304 stainless steels. A larger austenite grain size leads to a higher amount of martensite transformed and enhance both the plowing and adhesion effect during dry sliding. Therefore, both the surface COF and wear rate increase with the grain size of the austenite stainless steel.

2. Materials and Methods

2.1. Materials Preparation

The material used in the present study was a commercial cold rolled AISI 304 stainless steel block. The chemical composition of the steel is C-0.03, Mn-1.78, Cr-18.72, Ni-8.23, and Fe-balance (in wt.%). Square plate samples with a width of 25 mm and a thickness of 10 mm were cut from the block. The samples were then annealed at 1100 °C in a vacuum furnace filled with argon gas followed by water quenching to achieve a full austenite microstructure. Similar heat treatment process can be also found in literature [20]. The annealing time was varied from 1 h to 24 h to obtain full austenite microstructure with different initial grain sizes. Afterwards, the sample surfaces were grinded using SiC sandpapers with different grid numbers (from #180 to #800) followed by polishing with 3 micron diamond suspensions and 0.06 micron silica slurry. The initial surface roughness of the samples after

final polishing were measured by a 3-D surface profilometer (Rtec Instruments, San Jose, CA, USA) and the values of surface roughness of all the samples were less than 0.1 µm.

2.2. Friction and Wear Property Testing

Friction and wear properties of the 304 stainless steels were tested using a pin-on-plate sliding configuration, as shown in Figure 1. All the testing was carried out in ambient environment with a temperature of 20 °C and a relative humidity of about 20% on an R-tech muti-functional tribometer (Rtec Instruments, San Jose, CA, USA). The ball pin was made of alumina with a Vickers hardness of around 2000 VHN and a diameter of 6.5 mm. Dry sliding tests were conducted on the surface of the 304 stainless steels with different grain sizes. Applied loads were varied from 20 N to 150 N and a constant sliding velocity of 2 mm/s were adopted in the experiments. Each testing was repeated 5 times. The variation of COF with sliding distance was recorded and the worn morphologies were subjected to microstructure characterization.
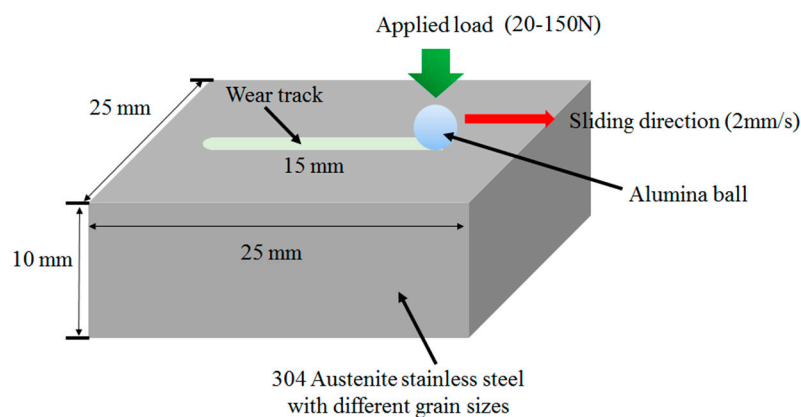
Figure 1. Schematic illustration of the pin-on-plate tribological testing of the 304 austenite stainless steel.

## 2.3. Microstructure Characterization and Hardness Testing

The wear behavior and microstructure evolution of the 304 stainless steel during sliding tests were characterized using a 3-D optical profilometer (Rtec Instruments, San Jose, CA, USA), JEOL-7100FT (JEOL Ltd., Tokyo, Japan) field emission scanning electron microscope (SEM) equipped with electron backscattered diffraction (EBSD). A particular focus was put on the wear track characterization. EBSD scans were performed on the samples tilted by 70° with a step size of 0.2 to 1.0 microns and the acquired data was analyzed with HKL Channel 5 data software (Oxford Instruments, Abingdon, UK). The surface micro-hardness of the 304 stainless steel samples with different annealing time before tribological testing were measured by a Wilson hardness test machine (Buehler, Lake Bluff, IL, USA) with a load of 500 g and a dwelling time of 10 s. Hardness tests were repeated 5 times for each sample.

3. Results

3.1. Initial Microstructure of the 304 Stainless Steel

Figure 2 shows the initial microstructure of the 304 stainless steel samples before tribological testing. The inverse pole figures (IPF) of the microstructure of the samples annealed at 1100 °C for 1, 2, 10, and 24 h are shown in Figure 2a–d, respectively. It can be seen that the grain size of the samples increases the annealing time. Mover, some annealing twins can be identified in the microstructure of the steel samples regardless of grain size. Figure 2e corresponds to the phase map of microstructure in Figure 2a. The phases with body-centered cubic (BCC), face-centered cubic (FCC), and hexagonal close-packed crystal (HCP) structure are marked by the red, green and yellow color, respectively. It is observed that the material possesses a full austenite microstructure after 1 h of annealing. The mean effective grain sizes of the samples with different annealing time were measured by the HKL Channel

5 software according to the ASTM-E2627 standard [21] and the results are shown in Figure 2f. It can be seen that the grain size increases from 25 to 92 μm as the annealing time increases from 1 h to 24 h.
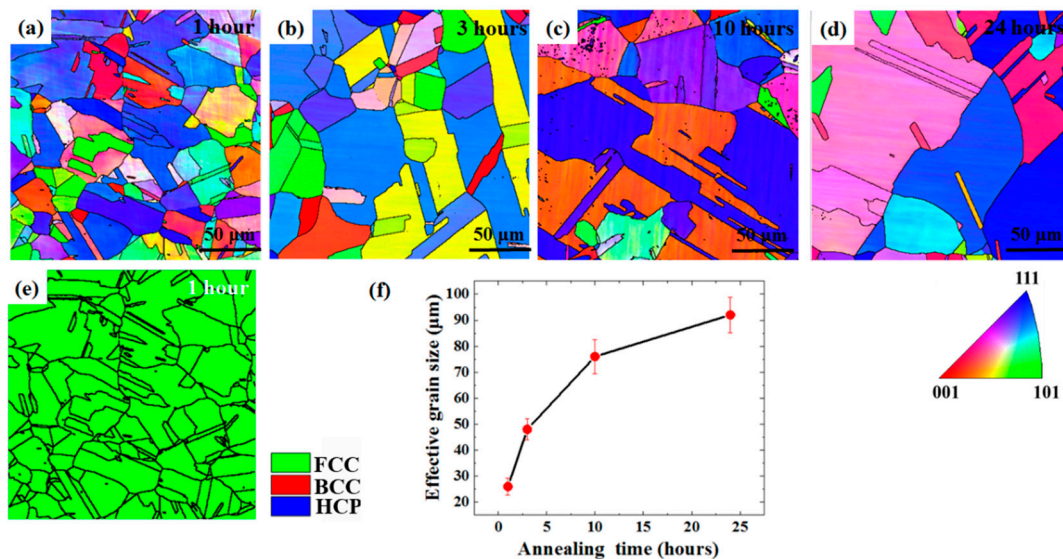
Figure 2. Inverse pole figure (IPF) map of the 304 stainless steels after annealing at 1100 °C for different time durations: (**a**) 1 h, (**b**) 3 h, (**c**) 10 h, and (**d**) 24 h. (**e**) Phase map of the microstructure corresponding to Figure 2a. (**f**) Variation of initial effective grain size of the 304 stainless steel samples with annealing time.

3.2. Effect of Austenite Grains Size on the COF

Figure 3 shows the effect of austenite grain size on the surface COF of 304 stainless steels measured by dry sliding tests. Figure 3a,b show the variation of COF with sliding distance for the sample with grain size of 25 and 92 μm, respectively. It can be found that the COF fluctuates around its mean value during dry sliding. Moreover, the increase of the applied load leads to the increase of COF values. For example, the mean value of COF increases from 0.058 to 0.071 as the applied load increases from 20 to 150 N for the sample with a grain size of 25 μm (Figure 3a). Similar trends also exist for the sample with a grain size of 92 μm, in which the mean value of COF increases from 0.074 to 0.21 as the applied load increases from 20 to 150 N (Figure 3b). Figure 3c shows the effect of the grain size on the mean values of COF measured by five different repeated testing. It was found that austenite grain size has a significant effect on the surface COF of austenite stainless steel, a refined grain size results in the decrease of COF, regardless of the applied loads. For instance, the surface COF decreases by 48% from 0.135 to 0.065 as the grain size decreases from 92 to 25 μm with an applied load of 80 N.
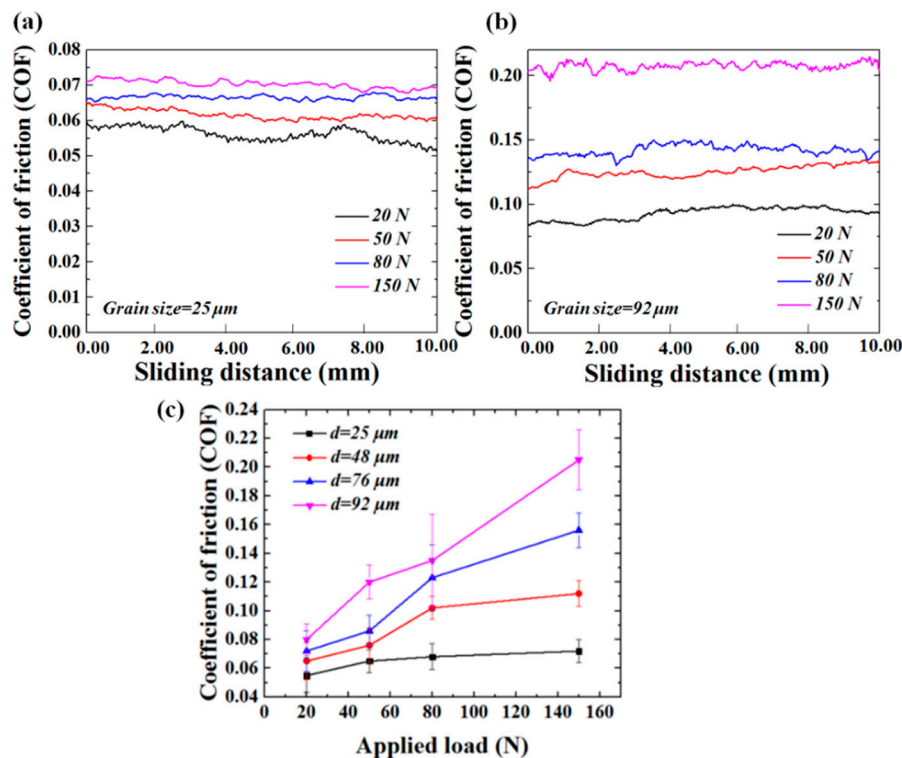
Figure 3. Variation of surface coefficient of friction (COF) with sliding distance of the 304 stainless steel sample with grain size of (**a**) 25 μm and (**b**) 92 μm at different applied loads. (**c**) Effect of grain size on the COF of the 304 stainless steels at different applied loads.

## 3.3. Effect of Austenite Grain Size on the Wear Behavior

The 3-D morphologies of the worn surfaces of the 304 stainless steels with different grain sizes after dry sliding with an applied load of 150 N are shown in Figure 4a–d. It can be seen that the surface was plastic deformed and materials were displaced to the two sides of the wear tracks due to the plowing effect [22]. With the increase of grain size, the depth of the wear track becomes deeper. A quantitative measurement of the profiles of the cross-sections of the wear tracks is shown in Figure 4e. It can be seen that the depth of the wear track increases from 1.75 to 2.25 μm as the grain size increases from 25 to 92 μm, indicating a weakened wear resistance of austenite stainless with larger grains. Moreover, the height of the edges of the wear track increases with the grain size due to the severer degree of plastic deformation. For instance, the height of the edge is 1.6 μm for the sample with a grain size of 92 μm, which is two times of that of the sample with a grain size of 25 μm. Since the wear rate is proportional to the cross-sectional area of the wear track, it can be calculated that the wear rates were reduced by around 30% as the grain size decreased from 92 to 25 μm. The surface micro-hardness values of the samples with different grain sizes are shown in Figure 4f. It can be seen that the surface micro-hardness of the 304 austenite steel increases with the decrease of grain size. For example, the Vickers hardness number (VHN) increases by 48% from 132 to 196 VHN as the grain size decreases from 92 to 25 μm.

Surface hardness plays an important role on the wear resistance of the metallic materials. According to the classical Archard's law [23], the wear volume, *V*, of a materials can be expressed as $V = \frac{LkW}{H}$, in which *L* is the sliding distance, *W* is the normal applied load and *H* is the hardness of the softer substrate subjected to wear. However, as the hardness of the 304 steel sample increases by 48% when the grain size decreases from 92 to 25 μm, the wear rates only decreases by around 30%. This observation indicates that apart from the surface micro-hardness, other factors, such as friction-induced martensitic transformation, might significantly influence the wear behavior of the austenite steel. A detailed discussion of the friction-induced martensitic transformation will be presented in Section 4.
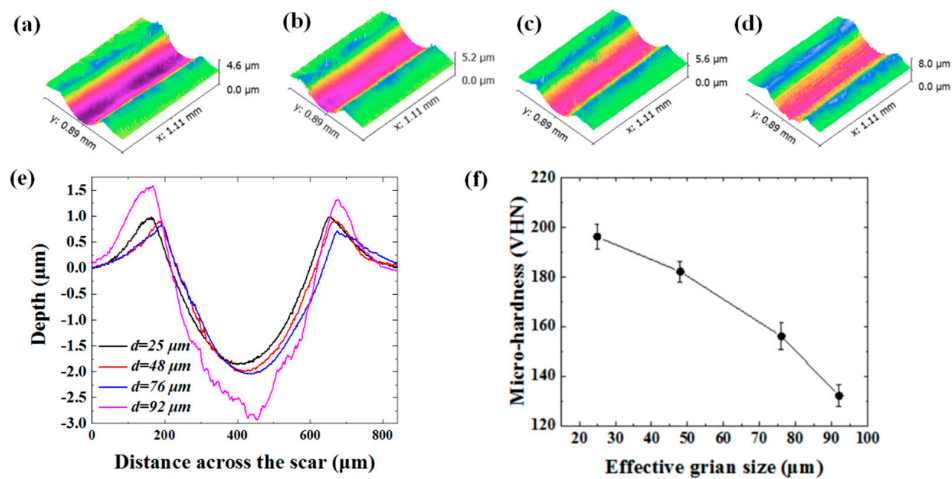
Figure 4. 3-D-surface profiles of the wear tracks of the 304 stainless steel samples with different grain sizes subjected to dry sliding with an applied load of 150 N: (**a**) d = 25 μm, (**b**) d = 48 μm, (**c**) d = 76 μm, and (**d**) d = 92 μm. (**e**) Cross-sectional profiles of the worn surfaces of the samples with different grain size. (**f**) The variation of surface micro-hardness with effective grain size for the 304 stainless steel samples.

To further characterize the effect of the grain size on the wear behavior of austenite stainless steel, the worn surfaces of the samples were examined by SEM. Figure 5 shows the surface morphologies of the samples with grain sizes of 48 and 92 μm after the dry sliding test with an applied of 80 N. It can be seen that the wear track consists of large amounts of micro-grooves. The width of the wear track for the sample with grain size of 48 μm is 234 μm (Figure 5a), which is smaller than that of the sample with grain size of 92 μm (312 μm in Figure 5c). Moreover, by checking the enlarged view of the wear track, it can be seen that both micro-cutting and surface delamination occurred during dry sliding of the sample with a grain size of 48 μm (Figure 5b). The surface delamination is an indication of severe adhesive wear, which has also been observed in other studies [24,25]. The surface delamination is more serious and some wear debris can be identified in the wear track of sample with a grain size of 92 μm as shown in Figure 5d, indicating the decreased wear resistance of 304 stainless steel with the increase of grain size. More specifically, it can be seen that by refining the austenite grain size, the adhesive wear component can be reduced.
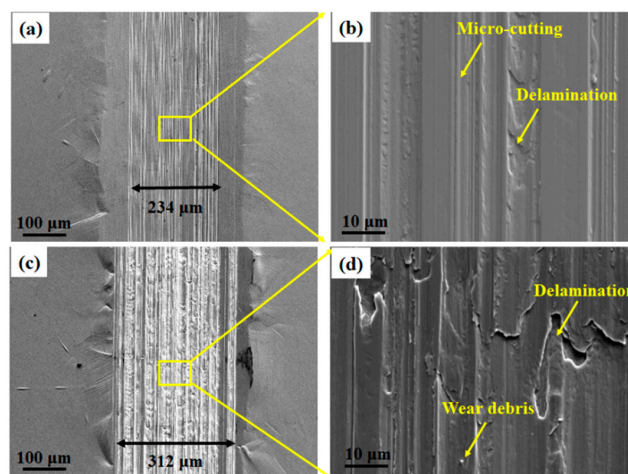

Figure 5. Scanning electron microscopy (SEM) images of the worn surfaces of the 304 stainless steel samples with a grain size of (**a**) 48 μm and (**c**) 92 μm after dry sliding test with an applied load of 80 N. (**b**,**d**) correspond to the enlarged view in the yellow box in (**a**) and (**c**) showing the wear mechanism.

4. Discussion

### 4.1. Frcition-Inudced Martensitic Tranformation

Friction-induced microstructural evolution makes a significant impact on the tribological behavior of metallic materials [8,26]. To investigate the microstructural evolution of 304 stainless steel during dry sliding, the wear track morphology was first examined by SEM. Figure 6 shows the SEM image of the worn surface of the steel sample with a grain size of 76 μm after dry sliding test with an applied load of 150 N. The middle area and front area of the wear track were examined and shown in Figure 6b,d, respectively. It can be seen that a considerable amount of slip traces was revealed besides the wear track, as shown in Figure 6b, due to the surface pile-up effect induced by the displacement of the materials. Figure 6c shows an enlarged view of the morphology in the front part of the wear track. It can be seen that the direction of the slip traces changes among different grains. Some slip-transfer effect can be identified in Figure 6c. Moreover, shear band intersection can be observed in Figure 6e, which can be acted as the nucleation site for stress-induced martensite [27]. Mateo et al. [28] showed that as the dislocation pile-up at the gran boundaries accumulate to a critical value, shear band forms and triggers the nucleation of martensite. Some surface wrinkles can be also identified in Figure 6d,e. The surface wrinkle may affect the tribological properties of 304 stainless steel through two different ways. First, it changes the surface morphology and affects the volume of the materials that continuous sliding need to shear [29]. Secondly, it might correspond to the hard martensite phase and affect the plasticity of the materials in front of the wear track [30]. All these two factors will significantly affect the plowing effect during dry sliding [31].
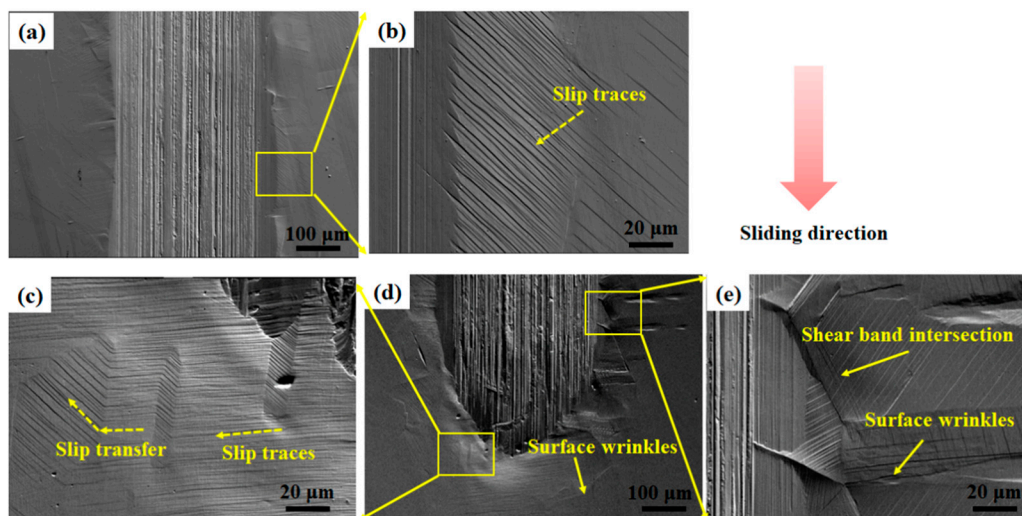
Figure 6. SEM images of the wear track of the 304 stainless steel with a grain size of 76 μm after dry sliding test with an applied load of 150 N: (**a**) Middle part of the war track and (**b**) the slip traces besides the wear track. (**d**) Front part of the wear track and enlarged view of some areas showing (**c**) slip trace and its transfer between grains and (**e**) shear band intersection and the formation of surface wrinkles.

To have a better understanding of the friction-induced martensitic transformation behavior, the front part of the wear tracks was analyzed by EBSD. Figure 7 shows the SEM image of the front part of the wear track of austenite steel sample with a grain size of 48 μm after dry sliding test with an applied load of 80 N. The area marked by yellow dash line in Figure 7a was analyzed by EBSD and the results are shown in Figure 7b–d. It can be seen that some lath-like martensite plates, which are marked by red color in the phase map in Figure 7b, were formed in the front part of the wear track. Moreover, it seems that martensite preferentially nucleated in some austenite grains with a {111} texture (marked by blue color in the IPF map in Figure 7c). One possible reason to account for this phenomenon might be the fact that those austenite grains have their {111} planes parallel to the sliding direction. Therefore,

dislocation slips on the {111} planes can be easily activated and trigger the formation of shear bands. Figure 7d shows the kernel average misorientation (KAM) map of the microstructure in the front part of the wear track; it can be seen that considerable high misorientation distributions occurs near the wear track. Moreover, high misorientation distributions can be also found near the martensite-austenite interface in the front part of the wear track. This local misorientation corresponds to the geometrically necessary dislocations (GND) induced by the martensitic formation and further affects the continuous deformation of austenite during dry sliding [32].
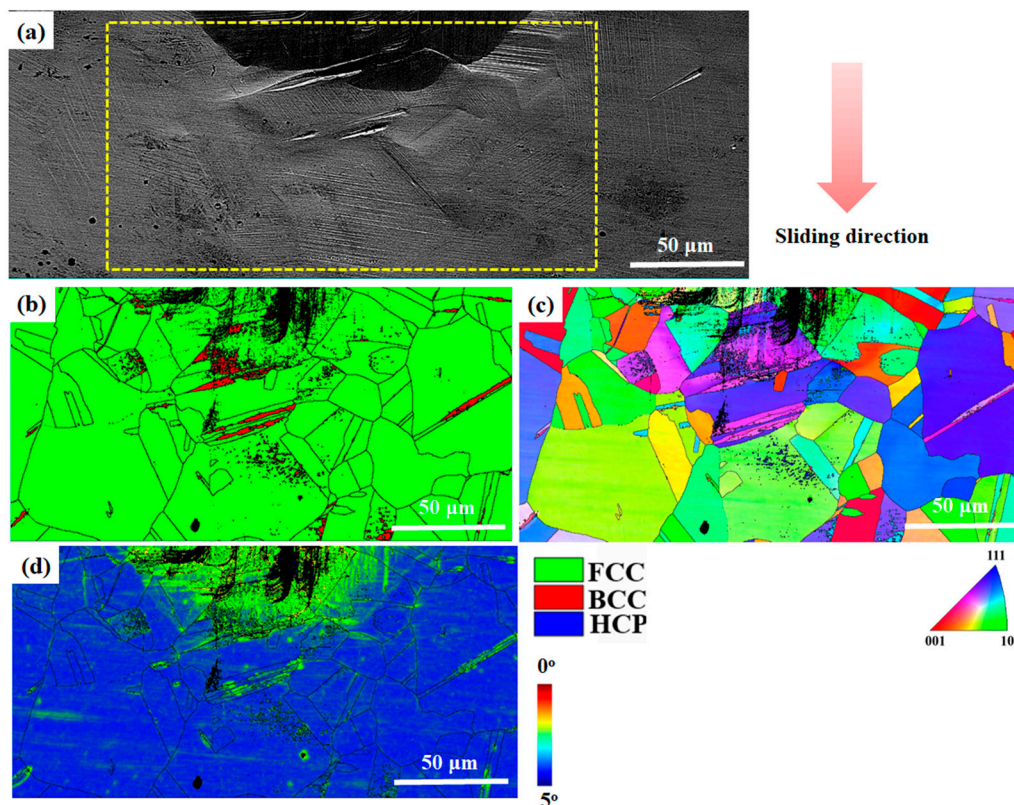

Figure 7. (**a**) SEM image the front part of the wear track of the 304 stainless steel with a grain size of 48 μm after dry sliding test with an applied load of 80 N. (**b**–**e**) Electron backscattered diffraction (EBSD) analysis of the transformation of austenite to martensitic in the front of wear track: (**b**) phase map, (**c**) inverse pole figure (IPF) map, and (**d**) kernel average misorientation (KAM) map.

In-depth analysis of the friction-induced martensite formation was carried out by SEM and EBSD with a fine step size. Figure 8a shows the SEM image of an area in the front part of the wear track. Three grains, G1, G2, and G3, with different slip trace directions are marked. EBSD analysis was performed on the area marked yellow dash line and shows that G1, G2, and G3 correspond to austenite grains, as shown in Figure 8b. Moreover, a lenticular shape of martensite, which corresponds to the surface wrinkle in G1 in Figure 8a, can be identified as martensite phase (BCC, in red), is marked as M. It was also observed that very few ε-martensite islands which have a HCP structure were also formed. ε-martensite was regarded as an intermediate phase between austenite and α'-martensite [33]. The intermediate step of austenite to ε-martensite with straining is due to the low Gibbs free energy difference between austenite and ε phases [34]. However, due to its negligible amount, it is not the focus of this study. Figure 8d shows the crystal unit cells of G1, G2, G3, and M. The slip planes of austenite grains with respect to the slip traces in Figure 8a are marked by a semi-transparent blue color, according to the analysis approach in previous research [35]. Schmid factors (SF) are calculated and the slip direction with the maximum SF are also shown in Figure 8d. It can be seen that the slip directions between G1 and G3 are almost parallel, which accounts for the large amount of slip-transfer between

G1 and G3 (Figure 8a) and good strain accommodation compatibility [36]. However, the slip directions between G1 and G3 shows a large deviation and may induce the stress concentration adjacent to the grain boundary. The stress concentration due to low strain accommodation compatibility may trigger the nucleation of martensite near the shear bands. Similar phenomenon was also observed in the research carried out by Wu et al. [37], in which they found that deformation-induced martensite in TRIP steels tends to nucleate only from the ferrite/austenite interfaces due to the large plastic incompatibility stress. Figure 8e,f show the {111} pole figure of the G1 and {110} pole figure of the M, it can be seen that {110} plane projections in the martensite phase somehow match with the {111} pole figure of M. Therefore, the orientation relationship between austenite and adjacent martensite follows the well-known Kurdjumov–Sachs (KS) relationship [38], i.e., $\{111\}_A//\{110\}_M$ and $\langle 101 \rangle_A//\langle 111 \rangle_M$. Moreover, the friction-induced martensite also exhibits some stress orientation dependent, as evidenced by its $\langle 101 \rangle$ somehow parallel to the sliding direction. Matsuoka et al. [39] showed that the deformation-induced martensite has a significant transformation texture where the $\langle 101 \rangle$ direction of martensite tends to be parallel to the tensile direction. However, such an argument may not be robust in this study due to complex stress state in the polycrystalline structure. Further analysis will be carried out on micro-scale sliding tests on single crystal austenite steel.
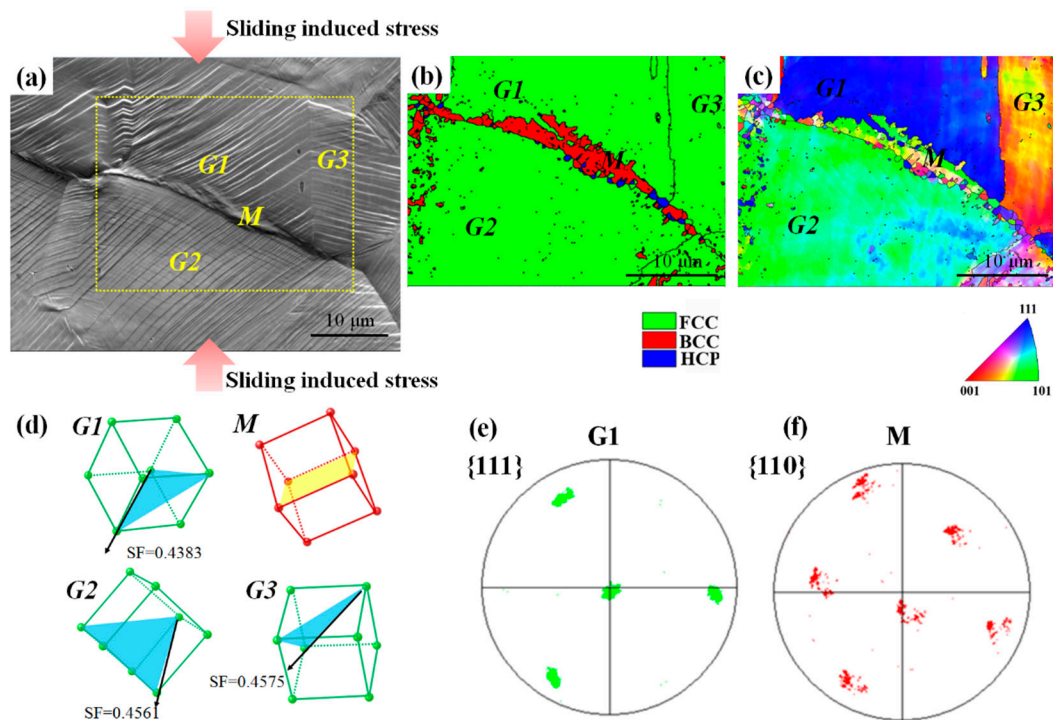
Figure 8. EBSD analysis showing the mechanism of friction-induced martensite transformation: (**a**) SEM image showing the different grains with different slip trace directions, (**b**) IPF map and (**c**) phase map of the area marked by yellow dash line in (**a**). (**d**) Crystal unit cells of the austenite grain G1-G3 and martensite grain M. The slip planes and slip directions with maximum SF in austenite crystals are marked. (**e**) {111} pole figure of the G1 grain. (**f**) {110} pole figure of the M grain.

To investigate the effect of grain size on the stress-induced martensitic transformation behavior, the microstructure in the front part of the wear track of austenite steel samples with different grain sizes are compared. Figure 9 shows the comparison of the microstructure in the front part of the wear track for the 304 stainless steel with a grain size of 48 (Figure 9a,b) and 92 µm (Figure 9c,d) after dry sliding test with an applied load of 150 N. According to the phase map, it can be seen that a considerable larger amount of martensite was formed in the front part of the wear track of steel sample with a grain size of 92 µm (Figure 9d) than that of steel with a grain size of 48 µm (Figure 9b). The shape of

martensite phase in the front part of the wear track in Figure 9a,b mostly shows a lath-like morphology while it turns irregular and consumes large volume of austenite parent grains, as shown in Figure 9c,d. Moreover, by comparing Figures 9b and 7c which correspond to the applied load of 80 N and 150 N in austenite stainless with a grain size of 48 μm, it can be seen that the volume of friction-induced martensite also increases with the applied load.
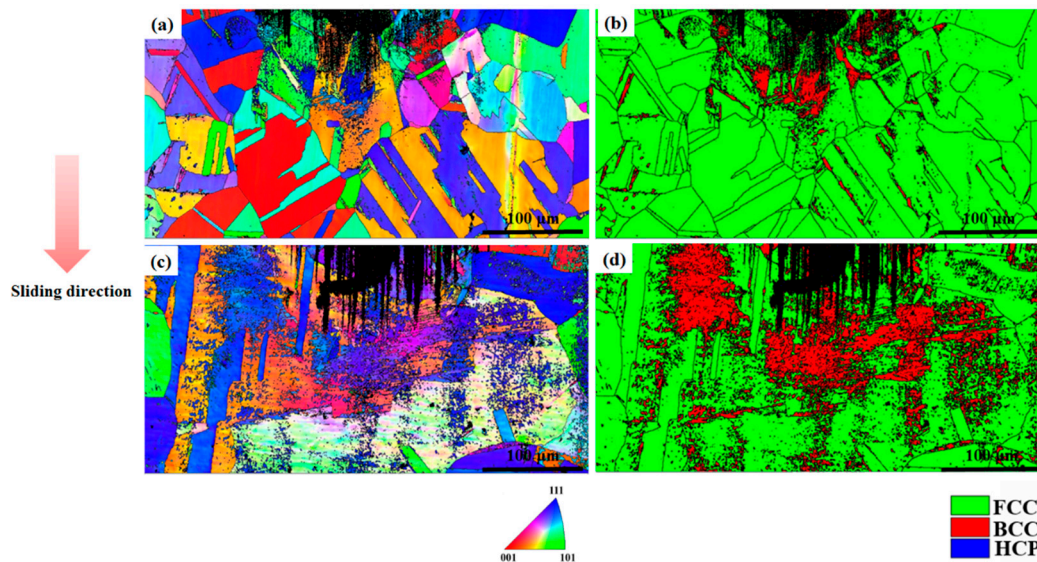
**Figure 9.** EBSD analysis of the friction-induced martensitic transformation on 304 stainless steel with grain size of (**a**,**b**) 48 μm and (**c**,**d**) 92 μm after dry sliding test with an applied load of 150 N. (**a**,**e**) are IPF maps while (**b**,**d**) are the corresponding phase maps.

The grain size dependence of deformation-induced martensitic transformation has been studied experimental and numerically by several researchers. Nohara et al. [40] showed that by decreasing the austenite grain size, the amount of strain-induced martensite decreases due to improved austenite stability. Levitas et al. [41] proposed that shear-band intersections are the major nucleation sites for stress or strain-induced martensitic transformation and the number of shear-band intersections determines the potential nucleation sites of martensite. In the constitutive model proposed by Stringfellow et al. [42], the number of intersections of shear bands N can be expressed as $N = K\left(N^{sb}\right)^n$, where N^{sb} is the number of the shear bands, n is a constant, K is a grain size-dependent parameter and can be described as: $k = \pi d^2/16$. Therefore, it seems that increasing the grain size leads to the improved chance of shear band intersection and promote the nucleation of martensite. In our study, as the normal load is applied by the alumina ball on the stainless steel sample, martensitic transformation occurs around the indentation to accommodate the local plastic deformation. Austenite steel sample with a larger grain size results in more martensite phases formed.

4.2. Proposed Mechanism

With the experimental observation and analysis carried out above, the mechanism responsible for the effect of grain size on the friction-induced martensitic transformation and the tribological performance of austenite stainless steel is proposed and schematically illustrated in Figure 10. When the alumina ball slides against the austenite stainless steel, the adhesion component and plowing component determines the values of COF and wear behavior [43]. As the adhesion component is a function of material pair, sliding environment, and real area of contact, it is expected that the variation of austenite grain size influences the adhesion component by affecting the real area of contact in the present study [44]. According to the experimental observations in Figures 4 and 5, it can be seen that austenite steel with a coarse grain leads to a wider wear track and a rougher contacting surface, leading

to a larger real area of contact, as shown in Figure 10b. Therefore, the increase of austenite grain size increases the adhesion component during dry sliding and lowers the wear resistance of austenite stainless. The plowing component depends on the degree of plastic deformation taking place at the asperity level [29,31]. It is presented in Figures 4 and 9 that a severer plastic deformation occurs in front of and besides the wear track for the sample with a coarser grain size, which is reflected by the larger amount of friction-induced martensite. Therefore, the amount of materials that the subsequent sliding needs to plow increases with the increase of grain size (Figure 10b). Moreover, as the amount of the martensitic transformed increases with the grain size, the larger volume fraction of martensite acting as a reinforcing phase will more effectively inhibit the movement of the alumina ball, further increasing the plowing component. These effects discussed above contribute to the friction and wear performance of austenite stainless steels.
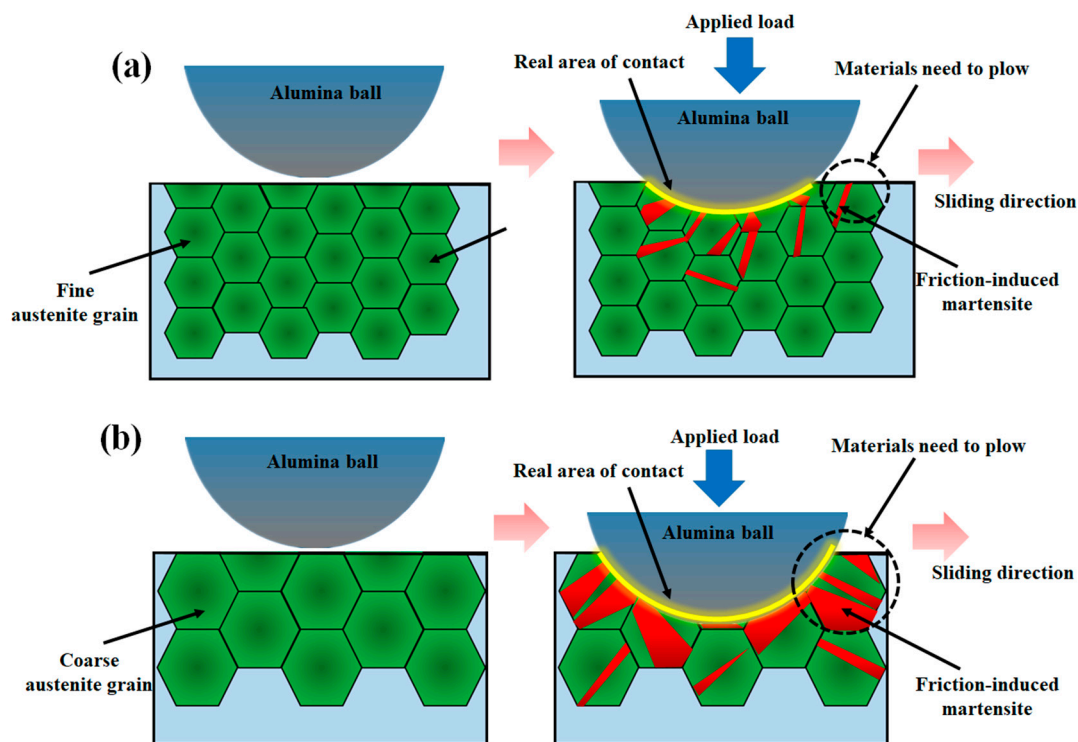
Figure 10. Schematic illustration of the mechanism of austenite grain size effect on the friction-induced martensitic transformation and tribological performance: (**a**) stainless steel with fine austenite grain size and (**b**) stainless steel with coarse austenite grain size.

5. Conclusions

The effect of grain size on the friction-induced martensitic transformation and tribological performance of 304 austenite stainless steels was systematically investigated in this study. The following conclusions can be drawn:

(1) Austenite grain size has a significant impact on the surface COF and wear resistance of 304 stainless steels. A larger austenite grain size results in a higher COF and lower wear resistance.

(2) Friction-induced martensitic transformation plays an important role during the dry sliding process and shows a grain size dependent behavior. A coarser austenite grain size leads to a higher amount of martensite transformed.

(3) Stress-induced martensite preferentially nucleates at the grain boundaries of the austenite with a {111} texture in the front of the wear track. The incompatibility of slip-transfer promotes the formation of martensite. The martensite variant selection tends to occur with its ⟨101⟩ direction along the sliding direction.

(4)   The mechanism responsible for the influence of austenite grain size on the COF and wear resistance of 304 austenite stainless steels is proposed. It is discussed that austenite grain size affects both the plowing and adhesion effect by affecting the amount of friction-induced martensite.

Author Contributions: Conceptualization, B.M., S.C. and S.W.; methodology, B.M. and S.C.; validation, B.M. and S.C.; formal analysis, B.M. and S.C.; writing—original draft preparation, B.M.; writing—review and editing, B.M., S.C. and S.W.; supervision, S.C.; project administration, S.C. and S.W.; funding acquisition, S.W.; All authors have read and agreed to the published version of the manuscript.

References

1.   Pereloma, E.; Edmonds, D.V. *Phase Transformations in Steels: Diffusionless Transformations, High Strength Steels, Modelling and Advanced Analytical Techniques*; Elsevier: Amsterdam, The Netherlands, 2012.
2.   Bhadeshia, H.K. TRIP-assisted steels? *ISIJ Int.* **2002**, *42*, 1059–1060. [CrossRef]
3.   Ajmani, S.; Bhattacharya, B.; Ghosh, C.; Roy, T.K. *Advanced High Strength Steel: Processing and Applications*; Springer: Singapore, 2018.
4.   Cobb, H.M. *Steel Products Manual: Stainless Steels*; Assn of Iron & Steel Engineers: Warrendale, PA, USA, 1999; p. 116.
5.   Berns, H.; Gavriljuk, V.; Riedner, S. *High. Interstitial Stainless Austenitic Steels*; Springer Science & Business Media: Berlin, Germany, 2012.
6.   Zhang, P.; Zhang, Y.; Liu, L.; Ren, X.; Zhang, Y.; Fang, Y.; Yang, Q. Numerical simulation on the stress field of austenite stainless steel during twin-roll strip casting process. *Comput. Mater. Sci.* **2012**, *52*, 61–67. [CrossRef]
7.   Yang, Z.; Naylor, M.; Rigney, D. Sliding wear of 304 and 310 stainless steels. *Wear* **1985**, *105*, 73–86. [CrossRef]
8.   Rigney, D.; Hirth, J. Plastic deformation and sliding friction of metals. *Wear* **1979**, *53*, 345–370. [CrossRef]
9.   Olofsson, U.; Telliskivi, T. Wear, plastic deformation and friction of two rail steels—A full-scale test and a laboratory study. *Wear* **2003**, *254*, 80–93. [CrossRef]
10. Fucheng, Z.; Tingquan, L. A study of friction-induced martensitic transformation for austenitic manganese steel. *Wear* **1997**, *212*, 195–198. [CrossRef]
11. Hua, M.; Xicheng, W.; Jian, L. Friction and wear behavior of SUS 304 austenitic stainless steel against Al_2O_3 ceramic ball under relative high load. *Wear* **2008**, *265*, 799–810. [CrossRef]
12. Lee, Y.-S.; Kondo, Y.; Okayasu, M. Friction-Induced Martensitic Transformation and Wear Properties of Stainless Steel under Dry and Wet Conditions. *Metals* **2020**, *10*, 743. [CrossRef]
13. Blondé, R.; Jimenez-Melero, E.; Zhao, L.; Schell, N.; Brück, E.; van der Zwaag, S.; Van Dijk, N. The mechanical stability of retained austenite in low-alloyed TRIP steel under shear loading. *Mater. Sci. Eng. A* **2014**, *594*, 125–134. [CrossRef]
14. Galindo-Nava, E.; Rivera-Díaz-del-Castillo, P. Understanding martensite and twin formation in austenitic steels: A model describing TRIP and TWIP effects. *Acta Mater.* **2017**, *128*, 120–134. [CrossRef]
15. Venables, J. The martensite transformation in stainless steel. *Philos. Mag. A J. Theor. Exp. Appl. Phys.* **1962**, *7*, 35–44. [CrossRef]
16. Zhang, Y.; Ding, H. Ultrafine also can be ductile: On the essence of Lüders band elongation in ultrafine-grained medium manganese steel. *Mater. Sci. Eng. A* **2018**, *733*, 220–223. [CrossRef]
17. Jin, J.-E.; Jung, Y.-S.; Lee, Y.-K. Effect of grain size on the uniform ductility of a bulk ultrafine-grained alloy. *Mater. Sci. Eng. A* **2007**, *449*, 786–789. [CrossRef]
18. Varma, S.; Kalyanam, J.; Murk, L.; Srinivas, V. Effect of grain size on deformation-induced martensite formation in 304 and 316 stainless steels during room temperature tensile testing. *J. Mater. Sci. Lett.* **1994**, *13*, 107–111. [CrossRef]
19. Bregliozzi, G.; Di Schino, A.; Kenny, J.; Haefke, H. The influence of atmospheric humidity and grain size on the friction and wear of AISI 304 austenitic stainless steel. *Mater. Lett.* **2003**, *57*, 4505–4508. [CrossRef]

20. Akita, M.; Uematsu, Y.; Kakiuchi, T.; Nakajima, M.; Tsuchiyama, T.; Bai, Y.; Isono, K. Effect of sensitization on corrosion fatigue behavior of type 304 stainless steel annealed in nitrogen gas. *Mater. Sci. Eng. A* **2015**, *640*, 33–41. [CrossRef]

21. ASTM International. *Standard Practice for Determining Average Grain Size Using Electron Backscatter Diffraction (EBSD) in Fully Recrystallized Polycrystalline Materials*; ASTM International: West Conshohocken, PA, USA, 2013.

22. Hsu, K.-L.; Ahn, T.; Rigney, D. Friction, wear and microstructure of unlubricated austenitic stainless steels. *Wear* **1980**, *60*, 13–37. [CrossRef]

23. Archard, J. Contact and rubbing of flat surfaces. *J. Appl. Phys.* **1953**, *24*, 981–988. [CrossRef]

24. Ceschini, L.; Chiavari, C.; Marconi, A.; Martini, C. Influence of the countermaterial on the dry sliding friction and wear behaviour of low temperature carburized AISI316L steel. *Tribol. Int.* **2013**, *67*, 36–43. [CrossRef]

25. Jourani, A.; Bouvier, S. Friction and wear mechanisms of 316L stainless steel in dry sliding contact: Effect of abrasive particle size. *Tribol. Trans.* **2015**, *58*, 131–139. [CrossRef]

26. Lychagin, D.V.; Filippov, A.V.; Novitskaia, O.; Chumlyakov, Y.I.; Kolubaev, E.A.; Sizova, O. Friction-induced slip band relief of-Hadfield steel single crystal oriented for multiple slip deformation. *Wear* **2017**, *374*, 5–14. [CrossRef]

27. Zhang, X.; Sawaguchi, T.; Ogawa, K.; Yin, F.; Zhao, X. Orientation dependence of variant selection and intersection reactions of ϵ martensite in a high-manganese austenitic steel. *Philos. Mag. Lett.* **2011**, *91*, 563–571. [CrossRef]

28. Mateo, A.; Sapezanskaia, I.; Roa, J.J.; Fargas, G.; Redjaïmia, A. Transmission of plasticity through grain boundaries in a metastable austenitic stainless steel. *Metals* **2019**, *9*, 234. [CrossRef]

29. Harries, K.A.; Zeno, G.; Shahrooz, B. Toward an improved understanding of shear-friction behavior. *ACI Struct. J.* **2012**, *109*, 835.

30. Straffelini, G.; Molinari, A.; Trabucco, D. Sliding wear of austenitic and austenitic-ferritic stainless steels. *Metall. Mater. Trans. A* **2002**, *33*, 613–624. [CrossRef]

31. Komvopoulos, K.; Saka, N.; Suh, N. Plowing friction in dry and lubricated metal sliding. *J. Tribol.* **1986**, *108*, 301–312. [CrossRef]

32. Souza Filho, I.; Zilnyk, K.; Sandim, M.; Bolmaro, R.; Sandim, H. Strain partitioning and texture evolution during cold rolling of AISI 201 austenitic stainless steel. *Mater. Sci. Eng. A* **2017**, *702*, 161–172. [CrossRef]

33. Cayron, C.; Barcelo, F.; de Carlan, Y. The mechanisms of the fcc–bcc martensitic transformation revealed by pole figures. *Acta Mater.* **2010**, *58*, 1395–1402. [CrossRef]

34. Abu-Farha, F.; Hu, X.; Sun, X.; Ren, Y.; Hector, L.G.; Thomas, G.; Brown, T.W. In situ local measurement of austenite mechanical stability and transformation behavior in third-generation advanced high-strength steels. *Metall. Mater. Trans. A* **2018**, *49*, 2583–2596. [CrossRef]

35. Di Gioacchino, F.; da Fonseca, J.Q. An experimental study of the polycrystalline plasticity of austenitic stainless steel. *Int. J. Plast.* **2015**, *74*, 92–109. [CrossRef]

36. Bieler, T.; Eisenlohr, P.; Zhang, C.; Phukan, H.; Crimp, M. Grain boundaries and interfaces in slip transfer. *Curr. Opin. Solid State Mater. Sci.* **2014**, *18*, 212–226. [CrossRef]

37. Wu, C.; Chang, C.; Chen, D.; Tu, J.; Huang, C. Microstructural characterization of deformation-induced martensite in an ultrafine-grained medium Mn advanced high strength steel. *Mater. Sci. Eng. A* **2018**, *721*, 145–153. [CrossRef]

38. Yardley, V.; Payton, E. Austenite–martensite/bainite orientation relationship: Characterisation parameters and their application. *Mater. Sci. Technol.* **2014**, *30*, 1125–1130. [CrossRef]

39. Matsuoka, Y.; Iwasaki, T.; Nakada, N.; Tsuchiyama, T.; Takaki, S. Effect of grain size on thermal and mechanical stability of austenite in metastable austenitic stainless steel. *ISIJ Int.* **2013**, *53*, 1224–1230. [CrossRef]

40. Nohara, K.; Ono, Y.; Ohashi, N. Composition and grain size dependencies of strain-induced martensitic transformation in metastable austenitic stainless steels. *Tetsu-to-Hagané* **1977**, *63*, 772–782. [CrossRef]

41. Levitas, V.; Idesman, A.; Olson, G.B. Continuum modeling of strain-induced martensitic transformation at shear-band intersections. *Acta Mater.* **1998**, *47*, 219–233. [CrossRef]

42. Stringfellow, R.; Parks, D.; Olson, G. A constitutive model for transformation plasticity accompanying strain-induced martensitic transformations in metastable austenitic steels. *Acta Metall. Mater.* **1992**, *40*, 1703–1716. [CrossRef]

43. Wanheim, T.; Bay, N.; Petersen, A. A theoretically determined model for friction in metal working processes. *Wear* **1974**, *28*, 251–258. [CrossRef]

44. Sharma, S.; Anand, B.; Krishna, M. Evaluation of sliding wear behaviour of feldspar particle-reinforced magnesium alloy composites. *Wear* **2000**, *241*, 33–40. [CrossRef]